AIAA SciTech Forum
6-10 January 2020, Orlando, FL
AIAA Scitech 2020 Forum

10.2514/6.2020-0248

Investigating Surface and Sub-Surface Damage in IM7/8552 via in-situ Synchrotron X-ray Computed Tomography

Imad A. Hanhan*, Michael D. Sangid†
Purdue University, West Lafayette, IN 47907

Francesco De Carlo‡
Argonne National Laboratory, Lemont, IL, 60439

Polymer matrix composites are popular in the aerospace industry due to their high strength to weight ratio. While they have become popular, understanding and predicting their specific damage evolution mechanisms remains a challenge especially in designing with damage tolerance criteria. One challenge often faced is the presence of surface damage either induced during manufacturing, machining, or service of a composite part. While many studies have investigated how quasi-static, low-velocity, and ballistic impact results in damage in the material, there remains a need to further understand the reduction in performance that results from such surface damage. In this work, micro-indentation was conducted on a unidirectional IM7/8552 laminate composite specimen to induce quasi-static impact damage that results in surface damage. The specimen was then loaded in tension to 33% of its expected failure load and imaged using synchrotron X-ray micro-computed tomography to qualitatively investigate the progression of surface damage into sub-surface damage. This work shows that at 33% of tensile failure load, surface damage propagates into delamination and fiber breakage of plies directly sub-surface. This work sheds light on the progression of surface damage at loads less than 50% of the ultimate strength of a unidirectional laminate composite.

I. Nomenclature

APS	=	Advanced Photon Source
DIC	=	Digital Image Correlation
μSXCT	=	Micro Synchrotron X-ray Computed Tomography

II. Introduction

Surface damage in composite materials is complex because it can encompass a number of different damage mechanisms, such as interlaminar and intralaminar delamination [1, 2], and fiber breakage [3]. While composite materials have a high strength to weight ratio, they can be sensitive to what may appear as minor damage - such as a tool drop during fabrication [4]. Specifically, it's often hard to detect foreign object damage in composite materials because unlike metals, there is often not a characteristic crater left behind. Furthermore, surface damage can vary depending on whether the damage was induced quasi-statically, at low-velocity impact, or at ballistic impact [5]. Overall, it is important to investigate and uncover the different damage modes that evolve from specific surface damage situations [6]. While work has been done to investigate the microstructural effects under certain impact conditions, it is also of interest to understand how damage from surface defects propagates under loading at the microstructural level [7–10]. Therefore, IM7/8552 was studied in this work using *μSXCT* at APS to investigate the progression of damage that was induced by micro-indentation at the surface of the specimen which was then monitored in-situ.

*Graduate Research Fellow, Aeronautics and Astronautics, 610 Purdue Mall, West Lafayette, IN 47907, AIAA Graduate Student Member
†Elmer F. Bruhn Associate Professor, Aeronautics and Astronautics, 610 Purdue Mall, West Lafayette, IN 47907, AIAA Sr. Member.
‡Group Leader (X-Ray Science Division), Advanced Photon Source, 9700 Cass Avenue, Lemont, IL 60439.

III. Materials and Methods

The carbon fiber laminate composite was a unidirectional IM7/8552 specimen fabricated and machined by the U.S. Army Research Laboratory for in-situ mechanical testing at the Advanced Photon Source (APS) at Argonne National Laboratory. In order to create a cylindrical specimen for symmetry when acquiring tomography, a thick laminate sheet was fabricated and then machined using a lathe into a cylindrical dog-bone shaped specimen, with dimensions shown in Figure 1. Due to the difficulty in machining composites, the smallest diameter that was achieved was 2.25 mm.

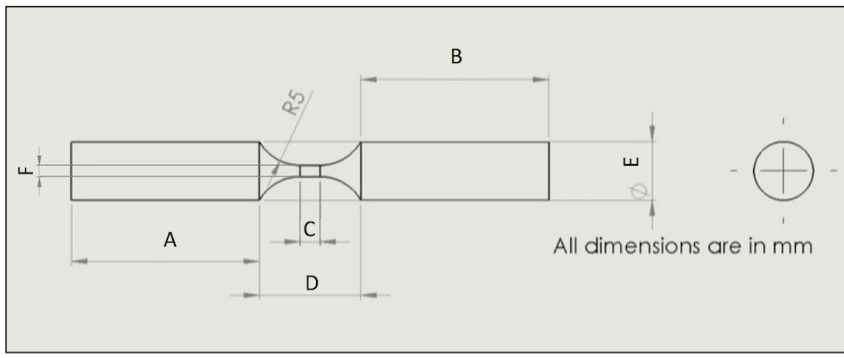

Parameter	Dimension (mm)
A	20
B	20
C	4.5
D	10.5
E	T 6.31 / B 6.36
F	2.25

Fig. 1 Specimen geometry with relevant dimensions.

In order to study the effect of surface damage, micro-indents were conducted on the surface of the specimen using a Leco hardness testing system. In order to do this, a custom dog-bone specimen holder was created to securely hold the cylindrical specimen in place while 3 micro-indents were applied longitudinally at each quadrant of the specimen's surface using a Vickers tip at 1000 g, 500 g, and 300 g held for 30 seconds at each indent. Specifically, the three micro-indents were evenly spaced in the length direction of the gauge section, and then the specimen was rotated 90°and indented again at each quadrant, resulting in 12 total indents. Indentation is ideally conducted on a smooth and flat surface; however since the surface in this case was rough and curved, indent geometry and depth of penetration was difficult to estimate and measure. An example of an indent conducted using 1000 g on the curved surface (which results in only one part of the image being in focus) can be seen in Figure 2.

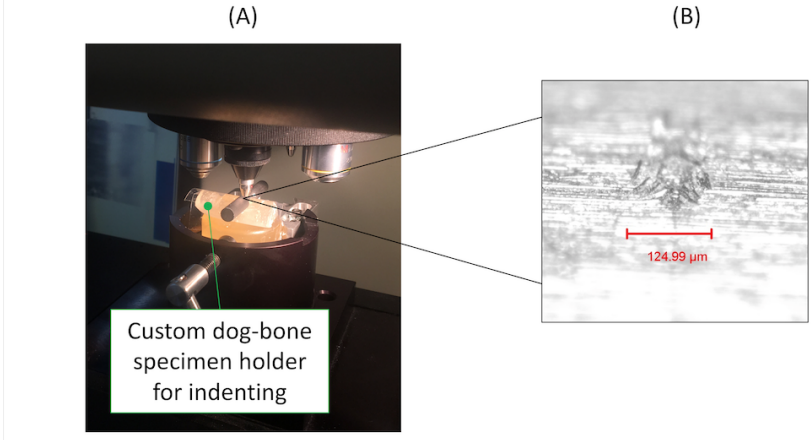

Fig. 2 The specimen's surface being indented in (A) and an optical micrograph of the indent in (B).

With the surface of the specimens indented, the tensile in-situ $\mu SXCT$ experiments were conducted at APS. An X-ray energy of 25 keV was used, the specimen was placed 75 mm away from the detector, and a 100 ms exposure time was used to acquire 1500 projections over 180°at a rotational speed of 0.5°per second. The experiment included three major data acquisition set-ups which are shown in Figure 3. The specimen was loaded in the miniature load frame and mounted onto a rotational stage which spins and allows for the capture of the X-ray projections, which were then

reconstructed using TomoPy [11] to output a 3D image with dimension 2560 x 2560 x 1240 pixels and a pixel size of 1.3 μm. Additionally, the load cell data was collected, saved, and used to determine the macroscopic stress that the specimen endured. Finally, a black and white pattern was painted on the surface of the specimen which was then monitored by an optical camera, allowing for macroscopic strain calculation through DIC.

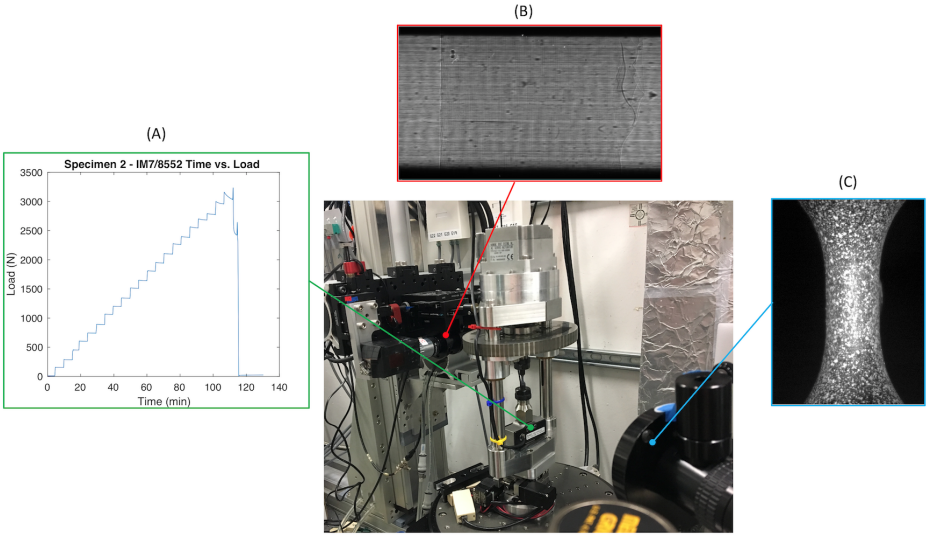

Fig. 3 Showing the experimental set-up where (A) is the load-time curve obtained by the load cell, (B) is an example X-ray projection acquired by the detector, and (C) is an optical image of the specimen's surface used for macroscopic strain measurements.

The reconstructed tomography images were then post-processed to improve the overall quality so indents can be identified and tracked across loading. The automated image processing was done iterating over each tomography image and is outlined in Figure 4. In Figure 4, the images are viewed in the YZ plane with the loading direction being up-down and the well aligned unidirectional fibers are seen as long vertical white streaks in the interior of the specimen.

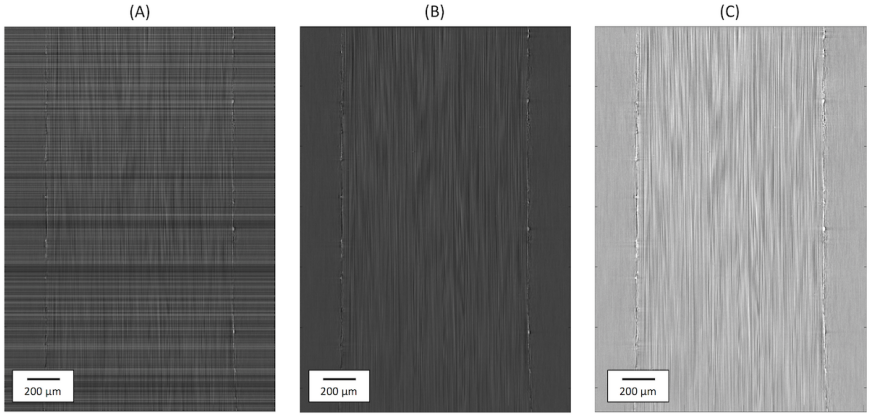

Fig. 4 Showing the sequence of image processing where (A) is the reconstructed image in the YZ plane, (B) is the result of slice-by-slice median scaling, and (C) is the result of hot-spot removal.

The tomography images were then examined for the micro-indents and of the 12 total indents, 8 were located in the tomography images. It is worth noting that due to the curvature and roughness of the specimen's surface, the quality of indentation was not consistent across all indents. For example, in some cases it is likely that the indenting tip began to slip along the curvature of the specimen resulting in a partial indent. Despite the challenging conditions when micro-indenting, the goal of inducing surface micro-damage was achieved, and 7 of the 8 located indents showed signs

of damage progression in the form of sub-surface fiber breakage and/or initiation of delamination when tracked to future loading steps.

IV. Results and Discussion

Two cases have been chosen for discussion, with one exhibiting sub-surface fiber breakage and the other exhibiting sub-surface fiber breakage and initiation of ply delamination. One case is shown in Figure 5, where the white pixels are related to paint agglomerating at the indent location where surface fibers were damaged during indentation (these damaged fibers can be seen in the optical microscopy image in Figure 2). It can be seen that after loading to 800 MPa, the indented region resulted in sub-surface fiber breakage which is seen in the tomography image of Figure 5 as dark intensity pixels directly sub-surface from the indent. In this case, the vertical displacement due to stretching of the specimen was not adjusted in the images in order to visually demonstrate the strain the material experienced.

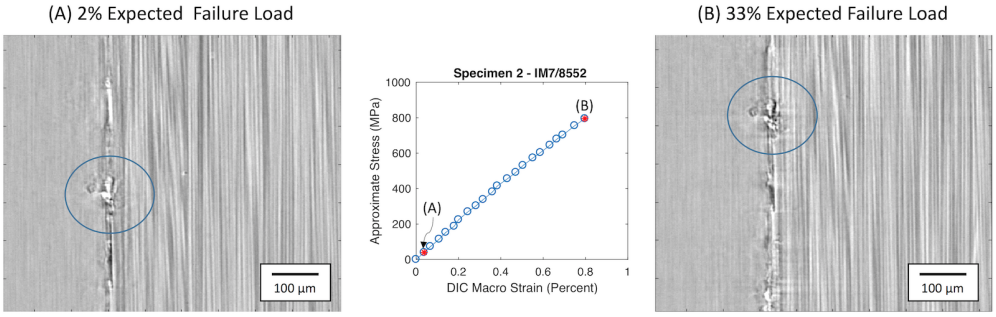

Fig. 5 Showing a micro-indent which resulted in sub-surface damage initiation in the form of micro-cracking and delamination at 33% of the failure load, where the vertical displacement is due to the deformation of the specimen.

Another case is provided in Figure 6, where the high intensity white pixels again correspond to paint agglomerating near the edge of the indent. In this case, the surface ply which was micro-indented lead to sub-surface fiber breakage and initiation of ply delamination which can be seen in the tomography image as a vertical line of dark pixels directly sub-surface. In this case, the vertical displacement due to stretching was adjusted to fit the entirety of both images. In general, this shows the capability of in-situ tomography to capture damage initiation resulting from micro surface damage, even when loading up to only 33% of the ultimate strength of the composite. Additional work is ongoing to create 3D renderings of the sub-surface damage at intermediate loading steps to provide additional insight into the damage evolution.

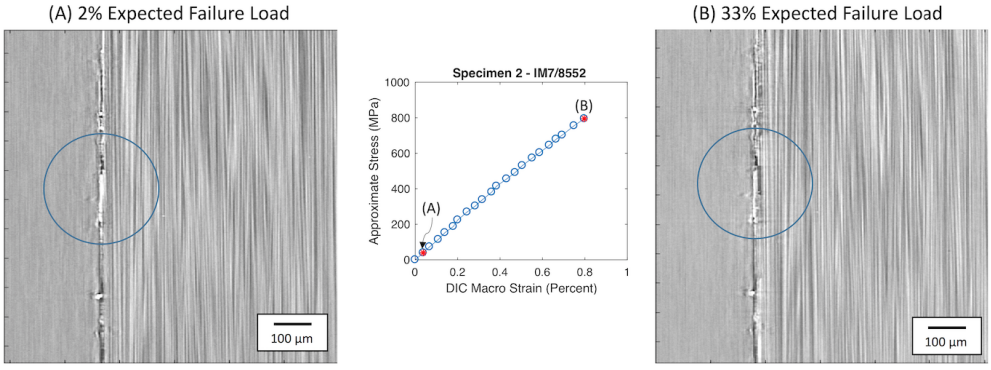

Fig. 6 Showing a micro-indent which resulted in sub-surface damage initiation in the form of micro-cracking and delamination at 33% of the failure load with the vertical displacement from deformation adjusted for a one-to-one comparison.

Acknowledgments

The authors gratefully acknowledge support from DARPA, Award No. HR0011-17-2-0069, under program manager Dr. Jan Vandenbrande, and the National Science Foundation CMMI MoM, Award No. 1662554, under program manager Dr. Siddiq Qidwai. Partial support for Imad Hanhan was provided by the National Science Foundation Graduate Research Fellowship Program under Grant No. DGE-1333468. The authors would like to acknowledge Dr. Daniel B. Knorr at the Army Research Lab for providing the material. The authors would also like to acknowledge Pavel Shevchenko, Ronald Agyei, and Rachel L. Roth for their assistance in acquiring and reconstructing X-ray tomography data and John Rotella for help with the micro-indentation. The use of the Advance Photon Source is granted by the US Department of Energy, Office of Science, and Office of Basic Energy Sciences under Contract No. DE-AC02 06CH11357.

References

[1] Gong, Y., Zhang, B., and Hallett, S. R., "Delamination migration in multidirectional composite laminates under mode I quasi-static and fatigue loading," *Composite Structures*, Vol. 189, No. September 2017, 2018, pp. 160–176. doi:10.1016/j.compstruct.2018.01.074, URL https://doi.org/10.1016/j.compstruct.2018.01.074.

[2] Czabaj, M. W., and Ratcliffe, J. G., "Comparison of intralaminar and interlaminar mode I fracture toughnesses of a unidirectional IM7/8552 carbon/epoxy composite," *Composites Science and Technology*, Vol. 89, 2013, pp. 15–23. doi:10.1016/j.compscitech.2013.09.008, URL http://dx.doi.org/10.1016/j.compscitech.2013.09.008.

[3] Schilling, P. J., Karedla, B. P. R., Tatiparthi, A. K., Verges, M. A., and Herrington, P. D., "X-ray computed microtomography of internal damage in fiber reinforced polymer matrix composites," *Composites Science and Technology*, Vol. 65, No. 14, 2005, pp. 2071–2078. doi:10.1016/j.compscitech.2005.05.014.

[4] Lapczyk, I., and Hurtado, J. A., "Progressive damage modeling in fiber-reinforced materials," *Composites Part A: Applied Science and Manufacturing*, Vol. 38, No. 11, 2007, pp. 2333–2341. doi:10.1016/j.compositesa.2007.01.017.

[5] Wen, H., Reddy, T., Reid, S., and Soden, P., "Indentation, Penetration and Perforation of Composite Laminate and Sandwich Panels under Quasi-Static and Projectile Loading," *Key Engineering Materials*, Vol. 141-143, 2009, pp. 501–552. doi:10.4028/www.scientific.net/kem.141-143.501.

[6] Hull, D., and Shi, Y. B., "Damage mechanism characterization in composite damage tolerance investigations," *Composite Structures*, Vol. 23, No. 2, 1993, pp. 99–120. doi:10.1016/0263-8223(93)90015-I.

[7] Abrate, S., "Impact on Laminated Composites: Recent Advances," *Applied Mechanics Reviews*, Vol. 47, No. 11, 1994, p. 517. doi:10.1115/1.3111065, URL http://appliedmechanicsreviews.asmedigitalcollection.asme.org/article.aspx?articleid=1395387.

[8] Tian, Z., and Swanson, S., "Residual Tensile Strength Prediction on a Ply-by-Ply Basis for Laminates Containing Impact Damage," *Journal of Composite Materials*, Vol. 26, No. 8, 1992, pp. 1193–1206. doi:10.1177/002199839202600807, URL http://journals.sagepub.com/doi/10.1177/002199839202600807.

[9] Hu, H., Wang, B. T., Lee, C. H., and Su, J. S., "Damage detection of surface cracks in composite laminates using modal analysis and strain energy method," *Composite Structures*, Vol. 74, No. 4, 2006, pp. 399–405. doi:10.1016/j.compstruct.2005.04.020.

[10] Sheikh-Ahmad, J., Urban, N., and Cheraghi, H., "Machining damage in edge trimming of CFRP," *Materials and Manufacturing Processes*, Vol. 27, No. 7, 2012, pp. 802–808. doi:10.1080/10426914.2011.648253.

[11] Gürsoy, D., De Carlo, F., Xiao, X., and Jacobsen, C., "TomoPy: A framework for the analysis of synchrotron tomographic data," *Journal of Synchrotron Radiation*, Vol. 21, No. 5, 2014, pp. 1188–1193. doi:10.1107/S1600577514013939.